Distinct proteomic CSF profiles in genetic frontotemporal lobar degeneration

Julie F. H. De Houwer,[1] Elise G. Dopper,[1] Renee van Buuren,[1] Marijke Stokkel,[2,3,4] Liset de Boer,[1] Tine Swartenbroekx,[1] Pam A. Boesjes,[1] Ana Rajicic,[1] Aitana Sogorb-Esteve,[5,6] Arabella Bouzigues,[5] Lucy L. Russell,[5] Phoebe H. Foster,[5] Eve Ferry-Bolder,[5] John C. van Swieten,[1] Lize C. Jiskoot,[1] Raquel Sanchez-Valle,[7] Robert Laforce,[8] Caroline Graff,[9,10] Daniela Galimberti,[11,12] Rik Vandenberghe,[13,14,15] Alexandre de Mendonça,[16] Pietro Tiraboschi,[17] Isabel Santana,[18,19] Alexander Gerhard,[20,21] Johannes Levin,[22,23,24] Benedetta Nacmias,[25,26] Markus Otto,[27] Maxime Bertoux,[28] Thibaud Lebouvier,[28] Simon Ducharme,[29,30] Chris R. Butler,[31,32] Isabelle Le Ber,[33,34,35] Elizabeth Finger,[36] Maria Carmela Tartaglia,[37] Mario Masellis,[38] James B. Rowe,[39] Matthis Synofzik,[40,41] Fermin Moreno,[42,43,44] Barbara Borroni,[45,46] Henrik Zetterberg,[5,47,48,49,50,51] Jonathan D. Rohrer,[1] Betty M. Tijms,[2,4] Yolande A. L. Pijnenburg,[2,4] Charlotte Teunissen[2,3,†] and Harro Seelaar[1,†]

[†]These authors contributed equally to this work.

Abstract

Fluid biomarkers to diagnose frontotemporal lobar degeneration (FTLD) are currently lacking. In this study, we aimed to identify proteomic changes in cerebrospinal fluid (CSF) associated with FTLD pathogenesis, focusing on signatures unique to different genetic groups. Additionally, we sought proteins distinguishing FTLD-spectrum disorders from controls.

To this end, we measured a comprehensive library of over 2900 proteins in CSF using proximity extension assay technology in two well-characterized FTLD cohorts. The discovery cohort, selected from the GENFI cohort, included 47 symptomatic pathogenic variant carriers (22 *C9orf72*, 14 *GRN,* 10 *MAPT* and 1 *TARDBP*), 124 presymptomatic pathogenic variant carriers (55 *C9orf72*, 44 *GRN*, 24 *MAPT* and 1 *TARDBP*) and 57 healthy non-carriers. The validation cohort comprised individuals clinically diagnosed with an FTLD-spectrum disorder (n = 132) and cognitively intact controls (n = 32). We assessed differentially abundant proteins using linear regression, adjusting for age and sex. Overrepresentation analysis was conducted for the three genetic groups using Gene

Ontology Biological Processes as ontology source. To develop diagnostic tools, we applied a LASSO regression, establishing two types of panels: one to distinguish individuals with an FTLD-spectrum disorder from controls (FTLD panel) and another to differentiate individuals with underlying TDP pathology from controls (TDP panel).

We observed 23 dysregulated proteins in symptomatic carriers. Of these, four were also significantly dysregulated (NEFL, TPM3, MSLN and DNM3) in the validation cohort. When focusing on genetic subgroups, 63 upregulated proteins were observed in symptomatic *MAPT* carriers, with enriched biological pathways linked to immune function. In symptomatic *C9orf72* carriers, four proteins – related to energy metabolism – were upregulated. When limiting symptomatic carriers to *GRN*, six proteins were dysregulated, with enriched pathways involved in neuronal development and projection. Notably, NEFL and TPM3 were consistently significant in all comparisons across both cohorts. We developed two diagnostic panels: one for FTLD and one for FTLD-TDP. The FTLD panel consisted of six proteins (NEFL, RBFOX3, NPTX1, TFF1, ENTPD5, and CNP). The TDP panel was made up of seven proteins (NEFL, RBFOX3, CBLN4, ENTPD5, CCL25, CNP, and MMP1). Both panels were successfully replicated in the validation cohort (AUC of 0.94 and 0.96 respectively).

This study highlights distinct proteomic signatures across FTLD genetic subgroups and their associated pathologies using a targeted proteomic approach. Additionally, we present two diagnostic panels—comprising both established and novel proteins—that effectively differentiate individuals with FTLD-spectrum disorders from healthy controls, offering promising avenues for improved clinical diagnosis.

Author affiliations:

1 Department of Neurology and Alzheimer Centre, Erasmus MC University Medical Centre, Rotterdam 3015 GD, The Netherlands

2 Amsterdam Neuroscience, Neurodegeneration, Amsterdam 1081 HV, The Netherlands

3 Neurochemistry Laboratory, Department of Laboratory Medicine, Amsterdam Neuroscience, Amsterdam UMC, Vrije Universiteit Amsterdam, Amsterdam 1081 HV, The Netherlands

4 Alzheimer Center Amsterdam, Neurology, Amsterdam UMC location VUmc, Vrije Universiteit Amsterdam, Amsterdam 1081 HV, The Netherlands

5 Dementia Research Centre, Department of Neurodegenerative Disease, UCL Queen Square Institute of Neurology, University College London, London WC1N 3AR, UK

6 UK Dementia Research Institute at University College London; WC1N 3BG, London, UK

7 Alzheimer's disease and Other Cognitive Disorders Unit, Neurology Service, Hospital Clínic, Institut d'Investigacións Biomèdiques August Pi I Sunyer, University of Barcelona, Barcelona 08036, Spain

8 Clinique Interdisciplinaire de Mémoire, Département des Sciences Neurologiques, CHU de Québec, and Faculté de Médecine, Université Laval, QC G1V 4G2, Canada

9 Department of Neurobiology, Care Sciences and Society,; Center for Alzheimer Research, Division of Neurogeriatrics, Bioclinicum, Karolinska Institutet, Solna 171 65, Sweden

10 Unit for Hereditary Dementias, Theme Inflammation and Aging, Karolinska University Hospital, Solna 171 76, Sweden

11 Department of Biomedical, Surgical and Dental Sciences, University of Milan, Milan 20122, Italy

12 Neurodegenerative Diseases Unit, Fondazione IRCCS Ospedale Maggiore Policlinico, Milan 20122, Italy

13 Laboratory for Cognitive Neurology, Department of Neurosciences, KU Leuven, Leuven 3000, Belgium

14 Neurology Service, University Hospitals Leuven, Leuven 3000, Belgium

15 Leuven Brain Institute, KU Leuven, Leuven 3000, Belgium

16 Faculty of Medicine, University of Lisbon, Lisbon 1649-028, Portugal

17 Fondazione IRCCS Istituto Neurologico Carlo Besta, Milano 20133, Italy

18 University Hospital of Coimbra (HUC), Neurology Service, Faculty of Medicine, University of Coimbra, Coimbra 3004-531, Portugal

19 Center for Neuroscience and Cell Biology, Faculty of Medicine, University of Coimbra, Coimbra 3004-504, Portugal

20 Division of Psychology Communication and Human Neuroscience, Wolfson Molecular Imaging Centre, University of Manchester, Manchester M20 3LJ, UK

21 Department of Nuclear Medicine, Center for Translational Neuro- and Behavioral Sciences, University Medicine Essen, Essen 45147, Germany

22 Department of Neurology, Ludwig-Maximilians Universität München, Munich 80802, Germany

23 German Center for Neurodegenerative Diseases (DZNE), Munich 81377, Germany

24 Munich Cluster of Systems Neurology (SyNergy), Munich 81377, Germany

25 Department of Neurofarba, University of Florence, Florence 50139, Italy

26 IRCCS Fondazione Don Carlo Gnocchi, Florence 50139, Italy

27 Department of Neurology, University of Ulm, Ulm 45 89081, Germany

28 Lille Neuroscience & Cognition U1172, University of Lille, Inserm, CHU Lille 59000, France

29 Douglas Mental Health University Institute, Department of Psychiatry, McGill University, Montreal, Québec H4H 1R3, Canada

30 McConnell Brain Imaging Centre, Montreal Neurological Institute, McGill University, Montreal, Québec H4H 1R3, Canada

31 Nuffield Department of Clinical Neurosciences, Medical Sciences Division, University of Oxford, Oxford OX3 7JX, UK

32 Department of Brain Sciences, Imperial College London, London SW7 2AZ, UK

33 Sorbonne Université, Paris Brain Institute – Institut du Cerveau – ICM, Inserm U1127, CNRS UMR 7225, AP-HP - Hôpital Pitié-Salpêtrière, Paris 75013, France

34 Centre de référence des démences rares ou précoces, IM2A, Département de Neurologie, AP-HP - Hôpital Pitié-Salpêtrière, Paris 75013, France

35 Département de Neurologie, AP-HP - Hôpital Pitié-Salpêtrière, Paris 75013, France

36 Department of Clinical Neurological Sciences, University of Western Ontario, London, ON N6A 3K7, Canada

37 Tanz Centre for Research in Neurodegenerative Diseases, University of Toronto, Toronto, ON M5G 1E8, Canada

38 Sunnybrook Health Sciences Centre, Sunnybrook Research Institute, University of Toronto, Toronto, ON M4N 3M5, Canada

39 Department of Clinical Neurosciences and Cambridge University Hospitals NHS Trust, University of Cambridge, Cambridge CB2 3EB, UK

40 Department of Neurodegenerative Diseases, Hertie-Institute for Clinical Brain Research and Center of Neurology, University of Tübingen, Tübingen 72076, Germany

41 Center for Neurodegenerative Diseases (DZNE), Tübingen 72076, Germany

42 Cognitive Disorders Unit, Department of Neurology, Hospital Universitario Donostia, 20014, San Sebastian, Spain

43 Biogipuzkoa Health Research Institute, Neurosciences Area, Group of Neurodegenerative Diseases, 20014 San Sebastian, Spain

44 Center for Biomedical Research in Neurodegenerative Disease (CIBERNED), Carlos III Health Institute, Madrid 28029, Spain

45 Department of Clinical and Experimental Sciences, University of Brescia, Brescia 15-25121, Italy

46 Molecular Markers Laboratory, IRCCS Istituto Centro San Giovanni di Dio Fatebenefratelli, Brescia 15-25125, Italy

47 Department of Psychiatry and Neurochemistry, Institute of Neuroscience and Physiology, the Sahlgrenska Academy at the University of Gothenburg; Mölndal 405 30, Sweden

48 Clinical Neurochemistry Laboratory, Sahlgrenska University Hospital; Mölndal 413 45, Sweden

49 Hong Kong Center for Neurodegenerative Diseases, Clear Water Bay; Hong Kong 999 077, China

50 Wisconsin Alzheimer's Disease Research Center, University of Wisconsin School of Medicine and Public Health, University of Wisconsin-Madison; Madison, WI 53726, USA

51 Centre for Brain Research, Indian Institute of Science, Bangalore 560012, India

Correspondence to: Dr Harro Seelaar

Erasmus Medical Centre (Erasmus MC)

Department of Neurology

Dr. Molenwaterplein 40

3015 GD Rotterdam, The Netherlands

E-mail: h.seelaar@erasmusmc.nl

Running title: CSF proteomic profiles in genetic FTLD

Keywords: frontotemporal dementia; dementia; familial; olink; proteome; proximity extension-based assay

Introduction

Frontotemporal lobar degeneration (FTLD) is a condition characterized by a wide range of clinical phenotypes and linked to diverse molecular pathologies and genetic underpinnings[1,2]. The most common clinical presentations are behavioural variant frontotemporal dementia (bvFTD), primary progressive aphasia (PPA), motor neurone disease (MND), corticobasal syndrome (CBS) and progressive supranuclear palsy (PSP)[3-7]. In addition, the vast majority of pathological substrates can be divided into two major categories: FTLD-TAR DNA-binding protein (FTLD-TDP) or FTLD with microtubule-associated protein tau (FTLD-tau)[8]. It is a highly heritable disorder with 20-30% of cases showing an autosomal dominant inheritance[9]. The three most important genes associated with FTLD are microtubule-associated protein tau *(MAPT),* progranulin *(GRN)* and chromosome 9 open reading frame 72 *(C9orf72)*. Additionally, several less common genes, including TAR DNA-binding protein (*TARDBP*), have also been associated with this condition.

Predicting the underlying pathology based solely on clinical phenotype is challenging, particularly in sporadic FTLD. However, certain phenotypes are more commonly linked to specific pathologies. For example, PSP is typically caused by FTLD-tau, while semantic variant PPA (svPPA) and motor neuron disease (MND) are strongly associated with FTLD-TDP[8]. Despite these associations, a definitive pathological and molecular diagnosis can only be made postmortem or through genetic testing. *C9orf72*, *GRN* and *TARDBP* are linked with FTLD-TDP, while *MAPT* is associated with FTLD-tau[9]. This well-established relationship with the underlying pathology makes genetic FTLD of particular interest, providing an ideal framework for studying these otherwise heterogeneous diseases.

The complex relationship between clinical presentations and underlying pathology not only complicates diagnosis but has also hampered the development of biomarkers. Despite this, significant progress has been made – for example – with neurofilament light chain (NEFL), a promising biomarker with a range of applications[10,11]. NEFL can aid in

distinguishing between FTLD and primary psychiatric disorders[12,13] and may serve as a proximity marker for symptom onset in genetic FTLD[14,15]. However, it cannot definitively diagnose FTLD nor differentiate between the various pathologies, because its levels are altered in many neurological disorders[16]. Recently, TDP-43 and 3R/4R tau in plasma-derived extracellular vesicles have been described[17], although these findings require replication. Considering upcoming clinical trials, the need for a biomarker capable of diagnosing the underlying pathology during life becomes increasingly pressing.

A promising strategy for the identification of novel fluid biomarkers are proteomics studies. Previous work in FTLD, utilizing antibody-based assays[18-20], mass-spectrometry methods[21,22] has identified several potential candidates. For instance, the neuronal pentraxins – NPTX1 and NPTX2 – have been discovered with an unbiased mass-spectrometry method in *GRN* carriers[21]. This finding was subsequently validated in independent cohorts[23,24], establishing NPTX2 as a recognized biomarker and underscoring the potential of this approach. A recent study, using untargeted mass spectrometry, identified distinct proteins associated with different genetic subgroups within the GENetic FTD Initiative (GENFI) cohort[22]. This further emphasizes the critical need for pathology- and gene-specific biomarkers.

High-throughput protein arrays, e.g., aptamer-based technologies, and immune-based proximity extension assays (PEA), enable the analysis of extensive protein libraries from small volumes of CSF samples. In Alzheimer's disease (AD), the use of PEA has generated promising results[25,26]. For example, using this innovative technique deeper insight into the disease's pathophysiology has been obtained, and clinically useful assays for distinguishing individuals with AD from healthy controls were developed and validated[25]. More recently, both an aptamer-based assay[27] and PEA[28] have been applied to FTLD, revealing proteomic signatures and disease-related pathways, underscoring the potential of these approaches for studying FTLD as well.

In this study, we measured over 2900 proteins in CSF using this PEA technology in two large, well-characterized FTLD cohorts, encompassing both genetic and sporadic cases. Our primary aim was to identify CSF proteomic changes that illustrate FTLD pathogenesis. By focusing on the different genetic groups, we aimed to uncover protein signatures that reflect the distinct pathophysiological processes driving each genetic group. Additionally, our secondary aim was to identify a subset of proteins that could distinguish individuals

with FTLD-spectrum disorders, with a particular focus on those with confirmed TDP pathology, from controls. However, due to the limited number of individuals with confirmed tau pathology, it was not feasible to identify a protein subset specific to this group.

Materials and methods

Ethics statement

Local ethics committees at each site approved the study. All participants were asked for written informed consent before inclusion in accordance with the World Medical Association Declaration of Helsinki.

Participants

In the discovery cohort, participants were recruited from the GENFI cohort across 13 sites (datafreeze 6). This cohort included CSF samples from 228 participants: 47 symptomatic pathogenic variant carriers (22 *C9orf72*, 14 *GRN,* 10 *MAPT* and 1 *TARDBP*), 124 presymptomatic pathogenic variant carriers (55 *C9orf72*, 44 *GRN*, 24 *MAPT* and 1 *TARDBP*) and 57 non-carriers (pathogenic variant-negative, first-degree family members). Data on CSF markers associated with Alzheimer's pathology ($A\beta_{42}$, tTau and $pTau_{181}$) was not available in the discovery cohort. The validation cohort (*n* = 164) included participants from the Erasmus MC University Medical Centre (*n* = 101) and the Amsterdam Dementia Cohort (ADC) (*n* = 63)[29]. The validation cohort comprised 132 individuals clinically diagnosed with an FTLD-spectrum disorder and 32 healthy controls. Participants were included if they met the diagnostic criteria for bvFTD, svPPA, non-fluent variant PPA (nfvPPA), logopenic variant PPA (lvPPA), CBS, PSP or MND[3-7]. A total of 79 participants underwent genetic analysis. Pathogenic variants were identified in 25 participants: 18 ***C9orf72*** hexanucleotide repeat expansions, 5 ***GRN*** and 2 ***TARDBP*** pathogenic variants. In addition, 8 individuals had pathological confirmation of either FTLD-TDP (*n* = 5) or FTLD-tau (*n* = 3) at autopsy[8]. CSF markers associated with Alzheimer's pathology ($A\beta_{42}$, tTau and $pTau_{181}$) were analysed using commercially available kits (ELISA Innotest Aβ(1–42), hTAUAg, pTau (181P; Fujirebio, Ghent) or Elecsys Aβ42, t-tau and p-tau (181P) CSF assays (Roche Diagnostics)). Individuals with a clinical FTLD phenotype, without pathological or genetic diagnosis, were only included if these markers did not indicate underlying Alzheimer's pathology. The control group consisted of individuals with subjective cognitive decline (*n* = 9) as well as healthy non-carriers (*n* = 23), all of whom had normal cognitive and laboratory test results.

All participants from both cohorts underwent a standardized assessment including a medical history, neurological examination, neuropsychological assessment, MRI and lumbar puncture. Individuals were excluded if a neurological or psychiatric comorbidity was present; data on systemic comorbidities (e.g., cancer) were not available. Participants were classified as symptomatic if they met consensus diagnostic criteria[3-7]. Control participants demonstrated normal performance on neuropsychological assessments and did not meet criteria for any neurological or psychiatric disorder.

CSF protein profiling

CSF samples were collected by lumbar puncture in polypropylene tubes and stored at -80°C at individual sites, according to international consensus guidelines[30]. Samples from other external sites were shipped to the Erasmus Medical Centre, Rotterdam, where they were stored and thawed at the day of aliquoting.

In both cohorts, CSF proteins were measured using the proprietary Olink® Explore 3072 platform which employs multiplex panels based on PEA technology (Olink® Proteomics Inc.), as previously described in detail[25,26]. Details on assay characteristics and quality control procedures are provided by the manufacturer and can be found on their website[31]. All samples were randomized over the plates and measured in one run. Complete protein data were available for every sample, with no missing values. Proteins were included for further analysis if they were above the limit of detection (LOD) in > 85% of samples and passed quality control. In addition, extreme outliers, defined as NPX values with a z-score exceeding +/- 5, were capped at a z-score of +/-5. Three proteins (IL6, CXCL8, and LMOD1) were measured across four panels, showing strong correlations between replicates (r range: 0.85 - 0.98). Of these, a single measurement was randomly selected from each set of replicates. In total, 2902 proteins were measured. In the discovery cohort, 1525 proteins were above LOD in more than 85% of samples, with 1516 unique proteins retained for further analysis. Among these, 324 extreme outliers (0.08%) were identified and capped. In the validation cohort, 1637 proteins were above LOD in over 85% of samples, and 1628 unique proteins were included for analysis; 446 extreme outliers (0.17%) were identified and capped.

Statistical Analysis

Differential protein abundance analysis

All statistical analyses were performed with R version 4.4.1. Basic demographics were compared between groups with a Mann-Whitney U test or a Kruskal-Wallis test with Dunn's post-hoc test for continuous variables and a chi-square test for categorical variables. To assess protein abundance, linear regression models were constructed for each protein. Protein concentration measurements served as the dependent variable, with the effect of the diagnostic group tested while adjusting for age and sex. To take disease severity into account, we first performed pairwise comparisons across the full discovery cohort: symptomatic carriers vs. non-carriers, symptomatic carriers vs. presymptomatic carriers, and presymptomatic carriers vs. non-carriers. These comparisons were then repeated separately within each genetic subgroup to explore mutation-specific effects. In the validation cohort, we compared individuals with FTLD to controls, and individuals with FTLD-TDP to controls. To determine whether the differentially abundant proteins are specific to FTLD or reflect broader changes across neurodegenerative disorders, we compared the summary statistics ($P < 0.05$) from previously published Olink® Explore 3072 datasets for AD[32] and α-synucleinopathies[33] with the differential abundant proteins of our discovery cohort. To assess the association between protein abundance and both cognitive function and disease severity we conducted a partial non-parametric correlation using the *ppcor* package (version 1.1), adjusting for age and sex. Analyses were limited to symptomatic carriers, first conducted in the full discovery cohort, and then repeated within each genetic subgroup. Tests included CDR Dementia Staging Instrument plus National Alzheimer's Coordinating Centre Frontotemporal Lobar Degeneration component (CDR® plus NACC FTLD) sum of boxes for disease severity, Mini Mental State Examination (MMSE) for global cognition and a neuropsychological battery measuring social cognition, attention, memory, language and executive function (Trail making Test (TMT) part B, TMTA, Stroop Colour Word Test (SCWT) interference card III, SCWT word (I), SCWT colour naming (II), Boston Naming Test (BNT), Benson figure copy and recall and Mini-SEA facial emotion recognition test). All analyses were false discovery rate (FDR)-corrected using the Benjamini-Hochberg method. The statistical significance threshold was set at a $P < 0.05$.

Overrepresentation analysis

We performed an overrepresentation analysis (ORA) in the discovery cohort, using the *ClusterProfiler* package (version 4.8.3), selecting Gene Ontology (GO) Biological Processes as ontology source. We performed ORA for three different genetic groups (e.g. *C9orf72*,

GRN, *MAPT*) separately with proteins with an unadjusted $P < 0.05$ as input. All proteins included in the statistical analysis were used as enrichment background. An FDR-corrected $P < 0.05$ was used to determine statistically significant enriched pathways.

Development of diagnostic panels

To identify a subset of proteins capable of distinguishing between individuals with FTLD and healthy controls, we utilized a feature selection algorithm named Stable Iterative Variable Selection (SIVS)[34,35]. This algorithm addresses inconsistency in model performance caused by embedded feature selection methods that do not robustly converge to the same feature space. Moreover, this algorithm enables substantial reduction of the feature space without compromising predictive accuracy. SIVS operates by performing multiple iterations of model construction using a specified method and aggregates selected features across iterations. We used the R package *sivs* (version 0.2.10) with a least absolute shrinkage and selection operator (LASSO) analysis as user-specified method and, measured proteins, age and sex as predictors. As input for the SIVS algorithm, we constructed two binomial logistic regression models within the discovery cohort: (i) all symptomatic carriers vs. non-carriers, and (ii) *C9orf72/GRN/TARDBP* symptomatic carriers vs. non-carriers, attributable to FTLD-TDP. The optimal combination of proteins was selected based on a user-specified strictness, which differed for each comparison. To validate these set of proteins, we constructed a LASSO logistic regression model limited to the selected proteins within the discovery cohort. This model was subsequently validated in the validation cohort by building comparable binomial logistic regression models (individuals with an FTLD-spectrum disorder vs. controls and individuals with confirmed TDP pathology vs. controls).

The predictive performance of all models was evaluated using Receiver Operating Characteristic (ROC) curves and corresponding Area Under the Curve (AUC) estimates. To compare the performance of each panel with CSF NEFL, we calculated ROC curves and AUC estimates for NEFL in parallel. Specifically, we generated one NEFL AUC using all FTLD individuals to match the FTLD panel, and a second NEFL AUC using only individuals with underlying TDP pathology to align with the TDP panel. We compared ROC curves between the panels and NEFL using the DeLong method[36] from the *pROC* package (version 1.18.5)[37].

Results

Demographics

Clinical characteristics of the discovery and validation cohorts are summarized in Table 1. In the discovery cohort, symptomatic carriers were significantly older than both presymptomatic carriers and non-carriers. Symptomatic carriers also had significantly lower MMSE scores and higher CDR® plus NACC FTLD scores compared to presymptomatic carriers and non-carriers. There was no difference in sex distribution between the three groups. Supplementary Table 1 summarizes clinical characteristics of the different genetic subgroups within the discovery cohort. In the validation cohort, individuals with FTLD were older than controls, with no difference in sex distribution between groups. As in the discovery cohort, individuals with FTLD had significantly lower MMSE scores and higher CDR® plus NACC FTLD scores compared to controls. Supplementary Table 2 summarizes clinical characteristics of the different pathological subgroups within the validation cohort.

CSF proteomics analysis

Discovery cohort

We first investigated which proteins differed between symptomatic carriers (*n*=47) versus non-carriers (*n*=57), and observed upregulated levels of 23 proteins (Fig. 1A, Supplementary Table 3A). None of these proteins were downregulated. Comparing symptomatic (*n*=47) and presymptomatic carriers (*n*=124) revealed seven proteins (TPM3, NEFL, MMP10, TFF1, MAP2K1, DNM3, FXN) that were upregulated in symptomatic carriers (Fig. 1B, Supplementary Table 3B). All these proteins also differed between symptomatic carriers and non-carriers. No proteins were differentially abundant between presymptomatic carriers (*n*=124) and non-carriers (*n*=57) (Supplementary Table 3C). Additionally, protein levels did not differ between symptomatic carriers with TDP pathology (e.g., *C9orf72*, *GRN*, *TARDBP*; *n*=37) and those with tau pathology (e.g., *MAPT*; *n*=10) (Supplementary Table 3D).

To explore specific genetic signatures, we performed comparisons restricted to each genetic group (e.g., *MAPT*, *C9orf72*, *GRN*) (Fig. 2). In symptomatic *MAPT* carriers (*n*=10) (Fig. 2A, Supplementary Table 4A), 63 proteins were upregulated compared to non-carriers (*n*=57). MMP10 and TFF1 also showed significant upregulation in symptomatic (*n*=10)

versus presymptomatic (*n*=24) *MAPT* carriers (Supplementary Table 4B). In symptomatic *C9orf72* repeat expansion carriers (*n*=22) (Fig. 2B, Supplementary Table 5A), four proteins (NEFL, TPM3, RBFOX3, ELAVL4) were upregulated relative to non-carriers (*n*=57). Comparing symptomatic (*n*=22) and presymptomatic (*n*=55) *C9orf72* carriers, only TPM3 exhibited dysregulation (Supplementary Table 5B). When limiting symptomatic carriers to *GRN* (*n*=14) (Fig. 2C, Supplementary Table 6A), three proteins were upregulated (NEFL, TPM3, DNM3) and three were downregulated (SEMA3G, GRN, NPTX2) compared with non-carriers (*n*=57). When comparing symptomatic (*n*=14) and presymptomatic *GRN* carriers (*n*=44), TPM3, NEFL, and NPTX2 remained significant (Supplementary Table 6B), whereas in presymptomatic *GRN* carriers (*n*=44) compared with non-carriers (*n*=57) GRN and SEMA3G were significantly downregulated (Supplementary Table 6C). Fig. 2D, illustrates protein abundance fold changes in a heatmap for significant proteins in symptomatic ***C9orf72*** and ***GRN*** carriers compared to non-carriers, as well as the top 10 significant proteins in symptomatic ***MAPT*** carriers compared to non-carriers. Among all comparisons, **NEFL** and **TPM3** consistently showed the greatest increases in abundance across symptomatic carriers, with highest levels observed in symptomatic ***GRN*** carriers. As expected, GRN is significantly decreased in symptomatic *GRN* carriers. However, the observed decrease in SEMA3G in these individuals represents a novel finding. Notably, **MMP10** exhibited a markedly greater increase in symptomatic ***MAPT*** carriers compared to the other genetic groups. To investigate whether underlying tau isoform influences MMP10 levels within *MAPT* carriers, we highlighted 3R, 4R, and 3R+4R tau isoforms in Supplementary Fig. 1. While MMP10 levels appeared higher in individuals with 3R isoform, further analysis was limited by the small sample size.

We examined whether protein levels were associated with measures of cognition and disease severity. In all symptomatic carriers, 515 proteins significantly correlated with TMTA (Supplementary Table 7). In addition, 75 proteins correlated with TMTA in symptomatic *GRN* carriers. No other significant correlations were observed for other cognitive or disease measures, or in other genetic subgroups (Supplementary Table 7).

Validation cohort

We repeated the differential abundance analysis in the validation cohort to replicate the findings of the discovery cohort. Comparing all FTLD individuals (*n*=132) with controls (*n*=32) identified 148 significantly dysregulated proteins, comprising seven that were upregulated and 141 that were downregulated (Supplementary Fig. 2A, Supplementary Table 8A). Four proteins, NEFL, TPM3, DNM3, and MSLN (Fig. 3A and 3C), were consistently

dysregulated in symptomatic individuals in both the discovery and the validation cohorts. Notably, MSLN displayed opposing fold changes—upregulated in the discovery cohort and downregulated in the validation cohort (Fig. 3C). Individuals with confirmed FTLD-TDP (*n*=30) showed 259 downregulated and five upregulated proteins compared to controls (*n*=32) (Supplementary Fig. 2B, Supplementary Table 8B). Examining proteins overlapping between individuals with confirmed FTLD-TDP pathology across both cohorts (Fig. 3B and 3D), we found that NEFL and TPM3 were dysregulated in both symptomatic *C9orf72* and *GRN* carriers from the discovery cohort and in individuals with confirmed FTLD-TDP in the validation cohort. In addition, GRN and NPTX2 were dysregulated in both symptomatic *GRN* carriers from the discovery cohort and in individuals with confirmed FTLD-TDP in the validation cohort. With only three participants having confirmed tau pathology in the validation cohort, a comparison between individuals with FTLD-tau and controls was not feasible. As a result, we could not replicate our findings from symptomatic *MAPT* carriers.

Comparison with Alzheimer's disease and Lewy body disease

We compared our findings with differentially abundant proteins across the AD spectrum (A^+T^- and A^+T^+)[32]. In total, 1,286 proteins were measured in both the AD dataset and our cohort. Of these, four proteins were significantly altered in symptomatic carriers and both AD groups (ITGB2, MAP2K1, FABP3, ATP5IF1; Fig. 4A). An additional three proteins were significantly changed in both symptomatic carriers and the A^+T^- group (CEP170, ELAVL4, DNM3; Fig. 4A), while five proteins were altered in both symptomatic carriers and the A^+T^+ group (CD69, MMP10, NEFL, RBFOX3, MSLN; Fig. 4A).

Examining the genetic subgroups, symptomatic *MAPT* carriers had nine proteins in common with both AD groups (ATP5IF1, CRKL, DTX3, FABP3, GLOD4, MAP2K1, NSFL1C, SDC4, TMSB10; Fig. 4B), two coinciding with A^+T^- (ABL1, DNM3), and eight appearing in both *MAPT* and A^+T^+ (CD163, CD209, CD69, LACTB2, MMP10, MSLN, NEFL, PHYKPL; Fig 4B). In addition, 40 proteins—predominantly inflammatory markers—were unique to symptomatic *MAPT* carriers. In symptomatic *C9orf72* carriers, ELAVL4 was shared with A^+T^-, while NEFL and RBFOX3 coincided with A^+T^+. In symptomatic *GRN* carriers, DNM3 appeared in common with A^+T^-, and NEFL with A^+T^+.

Next, we compared our findings with identified proteins differentially abundant in α-synucleinopathies, including both Parkinson's disease and dementia with Lewy bodies[33]. Of the 1,502 proteins measured in both datasets, none were significantly altered in both cohorts.

Overrepresentation analysis

We conducted an overrepresentation analysis within the discovery cohort, analysing each genetic group separately. In *MAPT* symptomatic mutation carriers, the top enriched terms pertain to the innate and adaptive immune system as well as cell activation (Supplementary Fig. 3A). For symptomatic ***C9orf72*** repeat expansion carriers, only one significant term was identified, which pertained to energy metabolism. Among *GRN* symptomatic carriers, the most significantly enriched terms are related to neuronal development, cell morphogenesis, and neuronal projection (Supplementary Fig. 3B). Notably, in *MAPT* symptomatic mutation carriers, most of the enriched terms are linked to upregulated proteins, whereas in *GRN* carriers, these terms are associated with downregulated proteins.

Development of diagnostic panels

We performed a feature selection analysis to determine which proteins could best distinguish between individuals with FTLD or individuals with FTLD-TDP and controls. We found that a panel of six proteins (NEFL, RBFOX3, NPTX1, TFF1, ENTPD5, CNP) most effectively discriminated between all symptomatic carriers (*n*=47) and non-carriers (*n*=57) in the discovery cohort (FTLD panel A; AUC = 0.98 [95% CI: 0.9798–0.9800]) (Supplementary Fig. 4). Three proteins – NEFL, RBFOX3 and TFF1 – were also significant in the univariate analysis; the other three – ENTPD5, NPTX1 and CNP – were not. When focusing on the genetic groups with underlying TDP-pathology (*n*=37), LASSO selected NEFL, RBFOX3, CBLN4, ENTPD5, CCL25, CNP and MMP1 (TDP panel A; AUC = 0.9978 [0.9977–0.9979]) (Supplementary Fig. 5). As NEFL was the primary contributor to both original panels, we repeated the analysis excluding NEFL to determine whether a comparable diagnostic accuracy could be reached using alternative protein combinations. For FTLD, a new six-protein panel—comprising NPTX1, RBFOX3, ATP5IF1, TFF1, DNM3, and MMP1—was identified (FTLD panel B; AUC = 0.98 [0.9799–0.9801]) (Supplementary Fig. 6). For TDP, a four-protein panel—RBFOX3, CBLN4, ATP5IF1, and MMP1—was selected (TDP panel B; AUC = 0.9749 [0.9749–0.97491]) (Supplementary Fig. 7). Notably, there was substantial overlap between panels A and B. In addition, most proteins, NEFL, RBFOX3, CBLN4, and MMP1,were already significant in the univariate analysis: NEFL and RBFOX3 in symptomatic versus non-carriers, and CBLN4 and MMP1 in FTLD-TDP versus controls. Due to the limited sample size, we could not conduct this analysis solely in individuals with FTLD-tau, nor could we create a panel to differentiate between individuals with FTLD-TDP and FTLD-tau.

After establishing the panels, we validated them using the independent validation cohort, with all panels showing excellent performance (Fig. 5A). FTLD panel A demonstrated high accuracy in distinguishing individuals with FTLD (*n*=132) from controls (*n*=32), achieving an AUC of 0.94 (95% CI: 0.88 – 1), compared to an AUC of 0.91 (0.93–0.98) for FTLD panel B, in which NEFL was excluded. In contrast, NEFL alone yielded an AUC of 0.89 (0.83 – 0.96) (Fig. 5B). Similarly, TDP panel A performed well in differentiating individuals with confirmed FTLD-TDP (*n*=30) from controls (*n*=32), with an AUC of 0.96 (0.92 – 1), while TDP panel B (without NEFL) has an AUC of 0.9 (0.81–0.99). NEFL alone achieved a slightly lower AUC of 0.85 (95% CI: 0.75–0.95) (Fig. 5B). The differences in performance between the panels and NEFL were not statistically significant (FTLD panel A versus B: *P*=0.387; FTLD panel A versus NEFL: *P*=0.366; FTLD panel B versus NEFL: *P*=0.819; TDP panel A versus B: *P*=0.173; TDP panel A: *P*=0.057; TDP panel B versus NEFL: *P*=0.488).

Discussion

In this study, we employed proximity extension assay technology to explore underlying pathophysiological processes in FTLD, using a CSF proteomic approach. We identified distinct and overlapping proteomic signatures across the three main genetic subgroups. In *MAPT* symptomatic carriers, 63 proteins were dysregulated, with a clear association to the adaptive and innate immune system. In *C9orf72* and *GRN* four and six proteins were dysregulated, respectively. Notably, NEFL and TPM3 were significantly upregulated in all comparisons of symptomatic individuals versus controls in both cohorts. Furthermore, we developed two protein panels—comprising six and seven proteins—that could effectively distinguish individuals with FTLD or FTLD-TDP from controls. These panels demonstrated excellent diagnostic accuracy in an independent cohort (AUC of 0.94 and 0.96, respectively), underscoring their potential as reliable diagnostic tools and valuable resources for advancing future research.

Both NEFL and TPM3 are significantly upregulated in all comparisons of symptomatic individuals versus controls across both cohorts. NEFL is a well-established, nonspecific marker of neurodegeneration and is among the fluid biomarkers currently used in clinical practice[12-15]. Interestingly, we found similar effect sizes for TPM3. In contrast to NEFL, TPM3 has not been extensively studied in the context of neurodegenerative diseases. As an actin-

associated protein, TPM3 regulates the structure and dynamics of actin filaments[38]. While it is predominantly expressed in muscle tissue[38], emerging evidence suggests that it also has a critical function in the actin cytoskeleton at the post synapse in the central nervous system[39,40]. Our findings are in line with a recent study reporting elevated CSF levels of TPM3 using mass spectrometry in a small cohort of symptomatic *GRN* carriers[41]. TPM3 was not part of the proteins included in the differential abundance analysis of the AD dataset by Pichet Binette *et al*[32]. However, given its upregulation across all comparisons, TPM3 may reflect axonal injury and neurodegeneration in a manner similar to NEFL. However, further research is needed to clarify its role in neurodegenerative diseases.

Symptomatic *MAPT* carriers exhibit a greater number of dysregulated proteins compared with other genetic groups (63 versus four and six). These results, however, should be interpreted with some caution given the small sample size (n = 10). Notably, many of these dysregulated proteins are associated with the innate and adaptive immune system. This is further reflected in the biological pathways linked to these proteins, which are predominantly enriched in immune response and cell activation pathways. While the role of neuroinflammation in neurodegenerative diseases is well-established[42,43], it is particularly striking that, in our study, this involvement is most pronounced in *MAPT*-related disease rather than in the other genetic subgroups. Interestingly, examining the overlap between significant proteins in symptomatic carriers and the AD spectrum reveals that several proteins are uniquely dysregulated in symptomatic *MAPT* carriers. This suggests that distinct proteins—and potentially different pathophysiological mechanisms—underlie *MAPT* and AD, despite both being tauopathies.

Among the dysregulated proteins in symptomatic *MAPT* carriers, MMP-10 stood out, showing a markedly greater increase in *MAPT* compared to the other genetic subgroups. It is a member of the matrix metalloproteinases (MMP) family, a group of zinc-dependent proteases involved in processes like extracellular matrix remodelling and neuroinflammation[44]. This prominent increase of MMP-10 and its role in inflammation are consistent with the core biological pathways identified in the proteomic signature of this genetic group in this study. Previous studies have consistently reported elevated CSF levels of MMP-10 among individuals with AD[26,45-47]. The increase in both AD and *MAPT*, in contrast to *GRN* and *C9orf72,* suggests MMP-10 might be a specific marker for underlying tau pathology. Nonetheless, a study using the same PEA technology found no significant MMP-10 dysregulation in atypical parkinsonian syndromes including PSP, a 4R-tauopathy, as well as in multiple system atrophy and Parkinson's disease, which are both α-

synucleinopathies[48]. This discrepancy may be explained by the fact that the majority of *MAPT* pathogenic variants included in this study result in a 3R + 4R tauopathy, similar to AD. Interestingly, visual inspection of the different tau isoforms and MMP-10 levels suggested higher levels in individuals with 3R-isoforms. Together, these findings highlights the need for further research to clarify the role of MMP-10 across tau isoforms and its potential to identify tau pathology in vivo, particularly in FTLD-tau with Pick's disease, a 3R tauopathy.

In symptomatic *C9orf72* carriers, ELAVL4 and RBFOX3 – both RNA-binding proteins – are significantly upregulated. ELAVL4, a member of the Hu protein family, is involved in regulation of RNA metabolism[49,50]. This protein has been extensively studied in neurodegenerative diseases, particularly in the context of amyotrophic lateral sclerosis (ALS), with multiple studies implicating ELAVL4 in familial ALS caused by pathogenic FUS variants[51-53]. In our study, ELAVL4 was significantly upregulated exclusively in *C9orf72*-related disease. However, other findings suggest its dysregulation might not be unique to this subgroup. For instance, cerebral organoids derived from V337M *MAPT* variant carriers also showed ELAVL4 upregulation[54]. This is further supported by its overlap with the A^+T^- group in the study by Pichet Binette *et al*.[32] RBFOX3 – encoding NeuN — is a well-established neuronal marker widely used in immunohistochemistry to assess neuronal health and neurodegeneration[55]. Together, these findings support the hypothesis that the dysregulation of ELAVL4 and RBFOX3 reflects broader RNA metabolism abnormalities in neurodegeneration, rather than being specific to *C9orf72*-related disease.

In *GRN* carriers, proteins and biological pathways related to overall synaptic integrity are observed, with evidence indicating the involvement of the neurovascular unit in these processes. A novel finding was the decrease in SEMA3G in presymptomatic and symptomatic *GRN* carriers. As a member of the semaphorin family, SEMA3G is part of a group of cell guidance cue proteins involved in cellular differentiation and migration[56]. It is secreted by endothelial cells and may function as a vascular-derived synaptic organizer, a potential role further supported by a knockout mouse model that exhibits impaired hippocampal-dependent memory[57]. Understanding how GRN haploinsufficiency leads to reduced SEMA3G levels—already evident in the presymptomatic stage—warrants further investigation. Moreover, in symptomatic *GRN* carriers,

the most enriched pathways are predominantly linked to neuronal development, cell morphogenesis, and neuronal projection, reflecting the critical role of synaptic integrity in cognitive functioning. Synaptic protein involvement in neurodegenerative diseases has been extensively studied, with NPTX2 recognized as a key synaptic marker in FTLD[23]. In our study, the largest fold-change was indeed observed in symptomatic *GRN* carriers. Beyond *GRN*-related disease, synaptic dysfunction plays a crucial role in FTLD-TDP. This is supported by the validation cohort, where CBLN4, a protein involved in synaptic plasticity[58-60], emerged as the top hit in individuals with FTLD-TDP. This aligns with the downregulation of CBLN4 observed in symptomatic *C9orf72* and *GRN* carriers in the study by Sogorb-Esteve *et al*[22].

When examining correlations between proteins and cognitive or disease measures, significant correlations were found with TMTA in symptomatic carriers, particularly in *GRN* carriers. The association of multiple proteins with attention—a relatively nonspecific feature in neurodegenerative diseases—may reflect the diverse clinical phenotypes observed across all symptomatic carriers, and particularly within *GRN* carriers. The lack of additional correlations could be due to the limited sample size of symptomatic carriers.

A striking observation was the opposing fold changes for MSLN —upregulated in symptomatic carriers in the discovery cohort and downregulated in individuals with FTLD in the validation cohort. In the discovery cohort, this upregulation may be driven by *MAPT* carriers, as MSLN was significantly upregulated in the *MAPT*-specific analysis. In contrast, the downregulation observed in the validation cohort could be influenced by individuals with underlying TDP pathology, given that the majority of this cohort has suspected TDP pathology based on pathological examination, genetic analysis or clinical phenotype. MSLN, a membrane-bound protein overexpressed in many tumours, has an as-yet poorly understood function, let alone in the central nervous system[61]. However, its strikingly divergent abundance across distinct pathologies has potential to advance the prediction of the underlying pathologies during life.

To facilitate the clinical translation of our findings, we developed two diagnostic panels to discriminate between individuals with FTLD or FTLD-TDP and healthy controls. Both panels demonstrated strong performance, which we successfully validated in an independent cohort, underscoring their potential. Given that NEFL was the primary driver of both panels, we conducted additional analyses excluding NEFL. These alternative panel versions also performed well, emphasizing the diagnostic value of other proteins beyond NEFL in FTLD. Although the overall performance of the diagnostic panels was comparable to that of NEFL alone, the composition of the panels offers insights into the distinct proteins and underlying pathophysiological processes involved in the disease. NEFL, RBFOX3, CNP and ENTPD5 were included in both panels. Given that both panels distinguish patients from controls, the inclusion of a nonspecific marker of neurodegeneration, such as NEFL or RBFOX3, is unsurprising. CBLN4 and CCL25, exclusive to the TDP panel, showed no significant dysregulation in *MAPT* carriers, indirectly implying a stronger association with TDP pathology than tau-related processes. Nonetheless, the specific roles of these proteins in TDP pathology require further investigation. In addition, it would be valuable to assess the panels' performance in distinguishing neurodegenerative diseases from primary psychiatric disorders or individuals with FTLD-tau, as well as in ALS and limbic-predominant TDP-43 encephalopathy.

In recent years, there has been increasing focus on precisely defining proteomic changes in FTLD and other neurodegenerative diseases, with various techniques being employed. For example, a recent study used untargeted mass spectrometry to identify proteomic changes within the same cohort as used in our study (e.g. GENFI cohort)[22]. The advantage of using multiple techniques to investigate the proteome – even within the same cohort – lies in their complementary characteristics. In our study, we used the PEA technology (Olink®), which relies on a predefined library of proteins, whereas mass spectrometry can offer an untargeted approach. However, PEA is particularly valuable for measuring low-abundance proteins and provides the advantage of being rapidly translatable to clinical settings, unlike mass spectrometry, which faces greater challenges in clinical implementation. Additionally, a recent study used an aptamer-based assay (SomaScan®) to measure over 4000 proteins in a genetic FTLD cohort[27]. Comparative studies of Olink® and SomaScan® suggest that the antibody-based Olink® platform offers higher specificity and stronger phenotypic associations, whereas SomaScan® provides

greater reproducibility and broader coverage of the proteome[62,63]. These distinct characteristics may account for divergent findings between platforms and underscore the value of applying multiple technologies for comprehensive proteomic profiling. The study by Saloner *et al*. uncovered several protein networks involved in FTLD, with a strong association between RNA metabolism proteins and the three genetic groups. However, as the authors noted, immune-related proteins were underrepresented in their panel. In contrast, our use of the Olink® platform provided broader coverage of immune-related proteins. This allowed us to uncover a strong connection between immune pathways and *MAPT*, adding an important dimension to the current proteomic landscape in FTLD. Moreover, while Saloner *et al.* explored protein co-expression networks, we focused on identifying individual proteins linked to the specific genetic subgroups. For example, we highlighted SEMA3G in *GRN*-related FTLD, which may serve as a marker of the neurovascular dysfunction reported in *GRN*[64]. Another example of the potential of these technologies comes from a recent study employing PEA, which measured a smaller set of proteins[28]. That work developed a 14-protein panel to distinguish individuals with FTLD from controls. In contrast, the strength of our study lies in the broader analysis of the CSF proteome and the development of a six-protein panel that achieves comparable performance.

A key strength of our study lies in the inclusion of two independent cohorts — a discovery cohort and a validation cohort — enabling us to replicate findings and evaluate the performance of diagnostic panels in an independent group. The discovery cohort included symptomatic and presymptomatic variant carriers as well as non-carriers of the GENFI study. This design leverages the well-established relationship between genetic FTLD and its underlying pathology, providing an ideal framework for studying and developing biomarkers, already in the presymptomatic stage of the disease. The validation cohort includes individuals across the full spectrum of FTLD, ensuring representation of real-world clinical practice.

Some limitations of this study should be considered. Only a limited number of differentially abundant proteins replicated between the discovery and validation cohorts. Although the inclusion of two cohorts is undoubtedly advantageous, interpretation is complicated by the inherent heterogeneity of the disease. Such heterogeneity has been highlighted by reported

differences between genetic and sporadic FTLD[65], as well as among the various TDP-43 subtypes[66]. To address this, replication in an independent FTLD cohort with genetic cases (for example, ALLFTD consortium) will be essential for validating and extending these results. In addition, age differences between controls and symptomatic individuals in the discovery cohort—less pronounced in the validation cohort due to the inclusion of individuals with subjective cognitive decline in the same age range—may also have contributed to the limited replication of differentially abundant proteins across cohorts. In addition, the small number of individuals with FTLD-tau limited comparisons between FTLD-TDP and FTLD-tau, replication of markers, and diagnostic panel development. A further limitation lies in the use of a targeted proteomics platform, which, while well-suited for high-throughput and reproducible analysis, captures only a part of the CSF proteome and may miss relevant markers that were not included. Untargeted mass spectrometry approaches or other targeted approaches (e.g.,apatamer based platforms) could complement these findings.

To conclude, using a targeted proteomic approach, we investigated the proteomic changes associated with FTLD within two large, well characterized cohorts. Our findings contribute to the growing body of evidence highlighting distinct proteomic signatures across genetic subgroups and underlying pathologies. We have demonstrated a contrast between the involvement of the adaptive immune system in *MAPT*-related disease and synaptic dysfunction in *GRN*-related disease. In addition, we show that PEA technology is a valuable tool to identify novel proteins and biological pathways relevant to therapeutic development, such as SEMA3G in *GRN*-related disease. Furthermore, we constructed two diagnostic panels capable of distinguishing individuals with an FTLD-spectrum disorder from healthy controls with potential as reliable diagnostic tools and valuable resources for advancing future research.

Data availability

Data can be accessed upon reasonable request to the corresponding author.

Acknowledgements

We thank all participants and their family members for taking part in this study. Several authors of this publication are members of the European Reference Network for Rare Neurological Diseases—Project ID no. 739510.

Funding

This project was funded by ZonMW Onderzoeksprogramma Dementie (TAP-Dementia project number 10510032120003, granted to C.E.T., B.M.T. and H.S.) and Alzheimer Nederland (WE.03-2022-07, granted to H.S. and C.E.T). J.C.V.S., L.C.J. and H.S. are supported by the Dioraphte Foundation grant 09-02-03-00, Association for Frontotemporal Dementias Research Grant 2009, Netherlands Organization for Scientific Research grant HCMI 056-13-018, ZonMw Memorabel (Deltaplan Dementie, project number 733 051 042), Joint Programme-Neurodegenerative Disease Research - GENFI-PROX (733051109), ZonMw Onderzoeksprogramma Dementie (YOD-INCLUDED, project number 10510032120002), EU Joint Programme-Neurodegenerative Disease (JPND) Research-GENFI-PROX, Alzheimer Nederland (WE.09-2022-05), Gieskes Strijbis Fonds and the Bluefield Project. R.S-V. is supported by Alzheimer's Research UK Clinical Research Training Fellowship (ARUK-CRF2017B-2) and has received funding from Fundació Marató de TV3, Spain (grant no. 20143810). C.G. received funding from EU Joint Programme-Neurodegenerative Disease Research-Prefrontals Vetenskapsrådet Dnr 529-2014-7504, EU Joint Programme-Neurodegenerative Disease Research-GENFI-PROX, Vetenskapsrådet 2019-0224, Vetenskapsrådet 2015-02926, Vetenskapsrådet 2018-02754, the Swedish FTD Inititative-Schörling Foundation, Alzheimer Foundation, Brain Foundation, Dementia Foundation and Region Stockholm ALF-project. D.G. received support from the EU Joint Programme—Neurodegenerative Disease Research and the Italian Ministry of Health (PreFrontALS) grant 733051042. R.V. has received funding from the Mady Browaeys Fund for Research into Frontotemporal Dementia. J.L. received funding for this work by the Deutsche Forschungsgemeinschaft German Research Foundation under Germany's Excellence Strategy within the framework of the Munich Cluster for Systems Neurology (EXC 2145 SyNergy—ID 390857198). M.O. has received funding from Germany's Federal Ministry of Education and Research (BMBF). SD received salary support from the Fonds de recherche du Québec – Santé. M.C.T. has received funding from the National Institute of Health, Michael J. Fox Foundation, Tannenbaum Institute for Science in Sport, Weston Brain Foundation. E.F. has received funding from a Canadian Institute of Health Research

grant #327387. M.M. has received funding from a Canadian Institute of Health Research operating grant and the Weston Brain Institute and Ontario Brain Institute. J.B.R. has received funding from the Wellcome Trust (103838; 220258), the Bluefield Project, and is supported by the Cambridge University Centre for Frontotemporal Dementia, the Medical Research Council (MC_UU_00030/14; MR/T033371/1) and the National Institute for Health Research Cambridge Biomedical Research Centre (NIHR203312). For the purpose of open access, the author has applied a CC BY public copyright licence to any Author Accepted Manuscript version arising from this submission. FM is supported by the Tau Consortium and has received funding from the Carlos III Health Institute (PI19/01637). BB is supported by JPND grant "GENFI-prox" (2019-02248). H.Z. is a Wallenberg Scholar and a Distinguished Professor at the Swedish Research Council supported by grants from the Swedish Research Council (#2023-00356, #2022-01018 and #2019-02397), the European Union's Horizon Europe research and innovation programme under grant agreement No 101053962, Swedish State Support for Clinical Research (#ALFGBG-71320), the Alzheimer Drug Discovery Foundation (ADDF), USA (#201809-2016862), the AD Strategic Fund and the Alzheimer's Association (#ADSF-21-831376-C, #ADSF-21-831381-C, #ADSF-21-831377-C, and #ADSF-24-1284328-C), the European Partnership on Metrology, co-financed from the European Union's Horizon Europe Research and Innovation Programme and by the Participating States (NEuroBioStand, #22HLT07), the Bluefield Project, Cure Alzheimer's Fund, the Olav Thon Foundation, the Erling-Persson Family Foundation, Familjen Rönströms Stiftelse, Stiftelsen för Gamla Tjänarinnor, Hjärnfonden, Sweden (#FO2022-0270), the European Union's Horizon 2020 research and innovation programme under the Marie Skłodowska-Curie grant agreement. No 860197 (MIRIADE), the European Union Joint Programme – Neurodegenerative Disease Research (JPND2021-00694), the National Institute for Health and Care Research University College London Hospitals Biomedical Research Centre, the UK Dementia Research Institute at UCL (UKDRI-1003), and an anonymous donor. J.D.R. is supported by the Bluefield Project and the National Institute for Health and Care Research University College London Hospitals Biomedical Research Centre, and has received funding from an MRC Clinician Scientist Fellowship (MR/M008525/1) and a Miriam Marks Brain Research UK Senior Fellowship. Several authors of this publication are members of the European Reference Network for Rare Neurological Diseases - Project ID No 739510. This work was also supported by the EU Joint Programme—Neurodegenerative Disease Research GENFI-PROX grant [2019-02248; to J.D.R., M.O., B.B., C.G., J.C.V.S. and M.S.

Competing interests

M.S. has received consultancy honoraria from Ionis, UCB, Prevail, Orphazyme, Biogen, Servier, reata, GenOrph, AviadoBio, Biohaven, Zevra, Lilly, and Solaxa, all unrelated to the present manuscript. J.B.R. has provided consultancy or advisory board input to Alector, Asceneuron, Astronautx, Astex, Cumulusneuro, Cerevance, Clinical Ink, Curasen, Eisai, and Wave, unrelated to the current work. S.D. has provided paid consultancy to QuRALIS, Eisai, Voyager Therapeutics and Eli Lilly and has received speaker fees from Eisai. S.D. is an SDMB member of Aviado Bio and IntelGenX. M.C.T. has received funding from the National Institute of Health, Michael J. Fox Foundation, Tannenbaum Institute for Science in Sport, Weston Brain Foundation. T.L. receives consultancy fees from Roche, Lilly, Biogen, and Eisai, which are directed entirely to his institution. R.V.'s institution has a clinical trial agreement (R.V. as PI) with Alector, AviadioBio, Denali, Eli Lilly, J&J, and UCB. R.V.'s institution has a consultancy agreement (R.V. as DSMB chair) with AC Immune. L.L.R. is a consultant for Prevail Therapeutics. H.Z. has served at scientific advisory boards and/or as a consultant for Abbvie, Acumen, Alector, Alzinova, ALZpath, Amylyx, Annexon, Apellis, Artery Therapeutics, AZTherapies, Cognito Therapeutics, CogRx, Denali, Eisai, Enigma, LabCorp, Merck Sharp & Dohme, Merry Life, Nervgen, Novo Nordisk, Optoceutics, Passage Bio, Pinteon Therapeutics, Prothena, Quanterix, Red Abbey Labs, reMYND, Roche, Samumed, ScandiBio Therapeutics AB, Siemens Healthineers, Triplet Therapeutics, and Wave, has given lectures sponsored by Alzecure, BioArctic, Biogen, Cellectricon, Fujirebio, LabCorp, Lilly, Novo Nordisk, Oy Medix Biochemica AB, Roche, and WebMD, is a co-founder of Brain Biomarker Solutions in Gothenburg AB (BBS), which is a part of the GU Ventures Incubator Program, and is a shareholder of MicThera (outside submitted work).

Supplementary material

Supplementary material is available at *Brain* online.

Appendix 1

GENFI Consortium Members

Rhian Convery, Martina Bocchetta, David Cash, Sophie Goldsmith, Kiran Samra, David L. Thomas, Thomas Cope, Maura Malpetti, Antonella Alberici, Enrico Premi, Roberto

Gasparotti, Emanuele Buratti, Valentina Cantoni, Andrea Arighi, Chiara Fenoglio, Vittoria Borracci, Maria Serpente, Tiziana Carandini, Emanuela Rotondo, Giacomina Rossi, Giorgio Giaccone, Giuseppe Di Fede, Paola Caroppo, Sara Prioni, Veronica Redaelli, David Tang-Wai, Ekaterina Rogaeva, Johanna Krüger, Miguel Castelo-Branco, Morris Freedman, Ron Keren, Sandra Black, Sara Mitchell, Christen Shoesmith, Robart Bartha, Rosa Rademakers, Jackie Poos, Janne M. Papma, Rick van Minkelen, Yolande Pijnenburg, Benedetta Nacmias, Camilla Ferrari, Cristina Polito, Gemma Lombardi, Valentina Bessi, Enrico Fainardi, Stefano Chiti, Mattias Nilsson, Henrik Viklund, Melissa Taheri Rydell , Vesna Jelic, Abbe Ullgren, Elena Rodriguez-Vieitez, Tobias Langheinrich, Albert Lladó, Anna Antonell, Jaume Olives, Mircea Balasa, Nuria Bargalló, Sergi Borrego-Ecija, Ana Verdelho, Carolina Maruta, Tiago Costa-Coelho, Gabriel Miltenberger, Frederico Simões do Couto, Alazne Gabilondo, Ioana Croitoru, Mikel Tainta, Myriam Barandiaran, Patricia Alves, Benjamin Bender, David Mengel, Lisa Graf, Annick Vogels, Mathieu Vandenbulcke, Philip Van Damme, Rose Bruffaerts, Koen Poesen, Pedro Rosa-Neto, Maxime Montembault , Raffaella Lara Migliaccio , Ninon Burgos, Daisy Rinaldi, Catharina Prix, Elisabeth Wlasich, Olivia Wagemann, Sonja Schönecker, Alexander Maximilian Bernhardt, Anna Stockbauer, Jolina Lombardi, Sarah Anderl-Straub, Adeline Rollin, Gregory Kuchcinski, Vincent Deramecourt, João Durães, Marisa Lima, Maria João Leitão, Maria Rosario Almeida, Miguel Tábuas-Pereira, Sónia Afonso, João Lemos.

References

1. Meeter LH, Donker Kaat L, Rohrer JD, van Swieten JC. Imaging and fluid biomarkers in frontotemporal dementia. Nat Rev Neurol. Jul 2017;13(7):406-419.

2. Grossman M, Seeley WW, Boxer AL, et al. Frontotemporal lobar degeneration. Nat Rev Dis Primers. Aug 10 2023;9(1):40.

3. Rascovsky K, Hodges JR, Knopman D, et al. Sensitivity of revised diagnostic criteria for the behavioural variant of frontotemporal dementia. Brain. Sep 2011;134(Pt 9):2456-77.

4. Gorno-Tempini ML, Hillis AE, Weintraub S, et al. Classification of primary progressive aphasia and its variants. Neurology. Mar 15 2011;76(11):1006-14.

5. Armstrong MJ, Litvan I, Lang AE, et al. Criteria for the diagnosis of corticobasal degeneration. Neurology. Jan 29 2013;80(5):496-503. doi:10.1212/WNL.0b013e31827f0fd1

6. Höglinger GU, Respondek G, Stamelou M, et al. Clinical diagnosis of progressive supranuclear palsy: The movement disorder society criteria. Mov Disord. Jun 2017;32(6):853-864.

7. Hardiman O, Al-Chalabi A, Chio A, et al. Amyotrophic lateral sclerosis. Nat Rev Dis Primers. Oct 5 2017;3:17071.

8. Mackenzie IR, Neumann M. Molecular neuropathology of frontotemporal dementia: insights into disease mechanisms from postmortem studies. J Neurochem. Aug 2016;138 Suppl 1:54-70.

9. Greaves CV, Rohrer JD. An update on genetic frontotemporal dementia. J Neurol. Aug 2019;266(8):2075-2086.

10. Meeter LH, Dopper EG, Jiskoot LC, et al. Neurofilament light chain: a biomarker for genetic frontotemporal dementia. Ann Clin Transl Neurol. Aug 2016;3(8):623-36.

11. van der Ende EL, Meeter LH, Poos JM, et al. Serum neurofilament light chain in genetic frontotemporal dementia: a longitudinal, multicentre cohort study. Lancet Neurol. Dec 2019;18(12):1103-1111.

12. Katisko K, Cajanus A, Jääskeläinen O, et al. Serum neurofilament light chain is a discriminative biomarker between frontotemporal lobar degeneration and primary psychiatric disorders. J Neurol. Jan 2020;267(1):162-167.

13. Ashton NJ, Janelidze S, Al Khleifat A, et al. A multicentre validation study of the diagnostic value of plasma neurofilament light. Nat Commun. Jun 7 2021;12(1):3400.

14. Rojas JC, Wang P, Staffaroni AM, et al. Plasma Neurofilament Light for Prediction of Disease Progression in Familial Frontotemporal Lobar Degeneration. Neurology. May 4 2021;96(18):e2296-e2312.

15. Giannini LAA, Seelaar H, van der Ende EL, et al. Clinical Value of Longitudinal Serum Neurofilament Light Chain in Prodromal Genetic Frontotemporal Dementia. Neurology. Sep 5 2023;101(10):e1069-e1082.

16. Bridel C, van Wieringen WN, Zetterberg H, et al. Diagnostic Value of Cerebrospinal Fluid Neurofilament Light Protein in Neurology: A Systematic Review and Meta-analysis. JAMA Neurol. Sep 1 2019;76(9):1035-1048.

17. Chatterjee M, Özdemir S, Fritz C, et al. Plasma extracellular vesicle tau and TDP-43 as diagnostic biomarkers in FTD and ALS. Nat Med. Jun 2024;30(6):1771-1783.

18. Remnestål J, Öijerstedt L, Ullgren A, et al. Altered levels of CSF proteins in patients with FTD, presymptomatic mutation carriers and non-carriers. Transl Neurodegener. Jun 23 2020;9(1):27.

19. Bergström S, Öijerstedt L, Remnestål J, et al. A panel of CSF proteins separates genetic frontotemporal dementia from presymptomatic mutation carriers: a GENFI study. Mol Neurodegener. Nov 27 2021;16(1):79.

20. Ullgren A, Öijerstedt L, Olofsson J, et al. Altered plasma protein profiles in genetic FTD - a GENFI study. Mol Neurodegener. Nov 15 2023;18(1):85.

21. van der Ende EL, Meeter LH, Stingl C, et al. Novel CSF biomarkers in genetic frontotemporal dementia identified by proteomics. Ann Clin Transl Neurol. Apr 2019;6(4):698-707. doi:10.1002/acn3.745

22. Sogorb-Esteve A, Weiner S, Simrén J, et al. Proteomic analysis reveals distinct cerebrospinal fluid signatures across genetic frontotemporal dementia subtypes. Sci Transl Med. Feb 5 2025;17(784):eadm9654.

23. van der Ende EL, Xiao M, Xu D, et al. Neuronal pentraxin 2: a synapse-derived CSF biomarker in genetic frontotemporal dementia. J Neurol Neurosurg Psychiatry. Jun 2020;91(6):612-621.

24. Sogorb-Esteve A, Nilsson J, Swift IJ, et al. Differential impairment of cerebrospinal fluid synaptic biomarkers in the genetic forms of frontotemporal dementia. Alzheimers Res Ther. Aug 31 2022;14(1):118.

25. Del Campo M, Peeters CFW, Johnson ECB, et al. CSF proteome profiling across the Alzheimer's disease spectrum reflects the multifactorial nature of the disease and identifies specific biomarker panels. Nat Aging. Nov 2022;2(11):1040-1053.

26. van der Ende EL, In 't Veld S, Hanskamp I, et al. CSF proteomics in autosomal dominant Alzheimer's disease highlights parallels with sporadic disease. Brain. Jun 22 2023;

27. Saloner R, Staffaroni AM, Dammer EB, et al. Large-scale network analysis of the cerebrospinal fluid proteome identifies molecular signatures of frontotemporal lobar degeneration. Nat Aging. Jun 2025;5(6):1143-1158.

28. Hok AHYS, Vermunt L, Peeters CFW, et al. Large-scale CSF proteome profiling identifies biomarkers for accurate diagnosis of frontotemporal dementia. Mol Neurodegener. Aug 27 2025;20(1):93.

29. van der Flier WM, Scheltens P. Amsterdam Dementia Cohort: Performing Research to Optimize Care. J Alzheimers Dis. 2018;62(3):1091-1111.

30. del Campo M, Mollenhauer B, Bertolotto A, et al. Recommendations to standardize preanalytical confounding factors in Alzheimer's and Parkinson's disease cerebrospinal fluid biomarkers: an update. Biomark Med. Aug 2012;6(4):419-30.

31. Olink. https://olink.com/

32. Pichet Binette A, Gaiteri C, Wennström M, et al. Proteomic changes in Alzheimer's disease associated with progressive Aβ plaque and tau tangle pathologies. Nat Neurosci. Oct 2024;27(10):1880-1891.

33. Pereira JB, Kumar A, Hall S, et al. DOPA decarboxylase is an emerging biomarker for Parkinsonian disorders including preclinical Lewy body disease. Nat Aging. Oct 2023;3(10):1201-1209.

34. Mahmoudian M, Venäläinen MS, Klén R, Elo LL. Stable Iterative Variable Selection. Bioinformatics. Dec 11 2021;37(24):4810-4817.

35. Venäläinen MS, Panula VJ, Eskelinen AP, et al. Prediction of Early Adverse Events After THA: A Comparison of Different Machine-Learning Strategies Based on 262,356 Observations From the Nordic Arthroplasty Register Association (NARA) Dataset. ACR Open Rheumatol. Oct 2024;6(10):669-677.

36. DeLong ER, DeLong DM, Clarke-Pearson DL. Comparing the areas under two or more correlated receiver operating characteristic curves: a nonparametric approach. Biometrics. Sep 1988;44(3):837-45.

37. Robin X, Turck N, Hainard A, et al. pROC: an open-source package for R and S+ to analyze and compare ROC curves. BMC Bioinformatics. Mar 17 2011;12:77.

38. Lambert MR, Gussoni E. Tropomyosin 3 (TPM3) function in skeletal muscle and in myopathy. Skelet Muscle. Nov 7 2023;13(1):18.

39. Stefen H, Chaichim C, Power J, Fath T. Regulation of the Postsynaptic Compartment of Excitatory Synapses by the Actin Cytoskeleton in Health and Its Disruption in Disease. Neural Plast. 2016;2016:2371970.

40. Tomanić T, Martin C, Stefen H, Parić E, Gunning P, Fath T. Deletion of the Actin-Associated Tropomyosin Tpm3 Leads to Reduced Cell Complexity in Cultured Hippocampal Neurons-New Insights into the Role of the C-Terminal Region of Tpm3.1. Cells. Mar 23 2021;10(3)

41. Pesämaa I, Müller SA, Robinson S, et al. A microglial activity state biomarker panel differentiates FTD-granulin and Alzheimer's disease patients from controls. Mol Neurodegener. Sep 29 2023;18(1):70.

42. Bright F, Werry EL, Dobson-Stone C, et al. Neuroinflammation in frontotemporal dementia. Nat Rev Neurol. Sep 2019;15(9):540-555. doi:10.1038/s41582-019-0231-z

43. Malpetti M, Rittman T, Jones PS, et al. In vivo PET imaging of neuroinflammation in familial frontotemporal dementia. J Neurol Neurosurg Psychiatry. Mar 2021;92(3):319-322.

44. Radosinska D, Radosinska J. The Link Between Matrix Metalloproteinases and Alzheimer's Disease Pathophysiology. Mol Neurobiol. Jun 27 2024;

45. Duits FH, Hernandez-Guillamon M, Montaner J, et al. Matrix Metalloproteinases in Alzheimer's Disease and Concurrent Cerebral Microbleeds. J Alzheimers Dis. 2015;48(3):711-20.

46. Boström G, Freyhult E, Virhammar J, et al. Different Inflammatory Signatures in Alzheimer's Disease and Frontotemporal Dementia Cerebrospinal Fluid. J Alzheimers Dis. 2021;81(2):629-640.

47. Martino Adami PV, Orellana A, García P, et al. Matrix metalloproteinase 10 is linked to the risk of progression to dementia of the Alzheimer's type. Brain. Jul 29 2022;145(7):2507-2517.

48. Jabbari E, Woodside J, Guo T, et al. Proximity extension assay testing reveals novel diagnostic biomarkers of atypical parkinsonian syndromes. J Neurol Neurosurg Psychiatry. Jul 2019;90(7):768-773.

49. Silvestri B, Mochi M, Garone MG, Rosa A. Emerging Roles for the RNA-Binding Protein HuD (ELAVL4) in Nervous System Diseases. Int J Mol Sci. Nov 23 2022;23(23)

50. Mulligan MR, Bicknell LS. The molecular genetics of nELAVL in brain development and disease. Eur J Hum Genet. Nov 2023;31(11):1209-1217.

51. De Santis R, Alfano V, de Turris V, et al. Mutant FUS and ELAVL4 (HuD) Aberrant Crosstalk in Amyotrophic Lateral Sclerosis. Cell Rep. Jun 25 2019;27(13):3818-3831 e5.

52. Garone MG, Birsa N, Rosito M, et al. ALS-related FUS mutations alter axon growth in motoneurons and affect HuD/ELAVL4 and FMRP activity. Commun Biol. Sep 1 2021;4(1):1025.

53. Silvestri B, Mochi M, Mawrie D, et al. HuD impairs neuromuscular junctions and induces apoptosis in human iPSC and Drosophila ALS models. Nat Commun. Nov 7 2024;15(1):9618.

54. Bowles KR, Silva MC, Whitney K, et al. ELAVL4, splicing, and glutamatergic dysfunction precede neuron loss in MAPT mutation cerebral organoids. Cell. Aug 19 2021;184(17):4547-4563 e17.

55. Duan W, Zhang YP, Hou Z, et al. Novel Insights into NeuN: from Neuronal Marker to Splicing Regulator. Mol Neurobiol. Apr 2016;53(3):1637-1647.

56. Carulli D, de Winter F, Verhaagen J. Semaphorins in Adult Nervous System Plasticity and Disease. Front Synaptic Neurosci. 2021;13:672891.

57. Tan C, Lu NN, Wang CK, et al. Endothelium-Derived Semaphorin 3G Regulates Hippocampal Synaptic Structure and Plasticity via Neuropilin-2/PlexinA4. Neuron. Mar 6 2019;101(5):920-937 e13.

58. Seigneur E, Polepalli JS, Südhof TC. Cbln2 and Cbln4 are expressed in distinct medial habenula-interpeduncular projections and contribute to different behavioral outputs. Proc Natl Acad Sci U S A. Oct 23 2018;115(43):E10235-E10244.

59. Favuzzi E, Deogracias R, Marques-Smith A, et al. Distinct molecular programs regulate synapse specificity in cortical inhibitory circuits. Science. Jan 25 2019;363(6425):413-417.

60. Liakath-Ali K, Polepalli JS, Lee SJ, Cloutier JF, Südhof TC. Transsynaptic cerebellin 4-neogenin 1 signaling mediates LTP in the mouse dentate gyrus. Proc Natl Acad Sci U S A. May 17 2022;119(20):e2123421119.

61. Hagerty BL, Takabe K. Biology of Mesothelin and Clinical Implications: A Review of Existing Literature. World J Oncol. Oct 2023;14(5):340-349.

62. Pietzner M, Wheeler E, Carrasco-Zanini J, et al. Synergistic insights into human health from aptamer- and antibody-based proteomic profiling. Nat Commun. Nov 24 2021;12(1):6822.

63. Katz DH, Robbins JM, Deng S, et al. Proteomic profiling platforms head to head: Leveraging genetics and clinical traits to compare aptamer- and antibody-based methods. Sci Adv. Aug 19 2022;8(33):eabm5164.

64. Gerrits E, Giannini LAA, Brouwer N, et al. Neurovascular dysfunction in GRN-associated frontotemporal dementia identified by single-nucleus RNA sequencing of human cerebral cortex. Nat Neurosci. Aug 2022;25(8):1034-1048.

65. Benussi A, Libri I, Premi E, et al. Differences and similarities between familial and sporadic frontotemporal dementia: An Italian single-center cohort study. Alzheimers Dement (N Y). 2022;8(1):e12326.

66. Pottier C, Küçükali F, Baker M, et al. Deciphering distinct genetic risk factors for FTLD-TDP pathological subtypes via whole-genome sequencing. Nat Commun. Apr 25 2025;16(1):3914.

Figure legends

Figure 1 Volcano plots displaying proteomic differences in the discovery cohort. Volcano plots display the proteomic differences between symptomatic carriers and non-carriers (**A**) as well as between symptomatic and presymptomatic carriers (**B**). These plots are based on a linear regression model, with age and sex as covariates. Differences were deemed significant if Benjamini-Hochberg adjusted *p*-values were <0.05. The grey dashed line indicates a *p*-value of 0.05, while the black dashed line represents an adjusted *p*-value of 0.05. The $\log_2$ fold change in protein abundance between groups is color-coded, with higher abundance shown in red.

Figure 2 Volcano plots and heatmap displaying proteomic changes in the genetic subgroups of the discovery cohort. Volcano plots show the proteomic differences in symptomatic *MAPT* (A), *C9orf72* (B) and *GRN* (C) variant carriers compared to non-carriers. These plots are based on a linear regression model, with age and sex as covariates. Differences were deemed significant if Benjamini-Hochberg adjusted *p*-values were <0.05.

The grey dashed line indicates a *p*-value of 0.05, while the black dashed line represents an adjusted *p*-value of 0.05. The $\log_2$ fold change in protein abundance between groups is color-coded, with higher abundance shown in red and lower abundance in blue.

(D) Heatmap illustrating the protein abundance fold changes for significant proteins in symptomatic ***C9orf72*** and ***GRN*** carriers compared to non-carriers, as well as the top 10 significant proteins in symptomatic ***MAPT*** carriers compared to non-carriers. The $\log_2$ fold change in protein abundance between groups is color-coded, with higher abundance shown in red and lower abundance in blue. * $p_{adjust} < 0.05$, ** $p_{adjust} < 0.01$, *** $p_{adjust} < 0.001$.

Figure 3 Venn diagram and heatmap displaying the overlapping proteomic signatures

Venn diagram showing the overlapping proteins between (**A**) individuals with an FTLD-spectrum disorder across the discovery and validation cohort (created in BioRender. De

Houwer, J. (2025) https://BioRender.com/bgn255j); and (**B**) between symptomatic *C9orf72* and *GRN* carriers from the discovery cohort and individuals with FTLD-TDP from the validation cohort (created in BioRender. De Houwer, J. (2025) https://BioRender.com/uzklaw9). Heatmap illustrating the protein abundance fold changes for the overlapping proteins between (**C**) individuals with an FTLD-spectrum disorder across the discovery and validation cohort, and (**D**) between symptomatic *C9orf72* and *GRN* carriers from the discovery cohort and individuals with FTLD-TDP from the validation cohort. * $p_{adjust} < 0.05$, ** $p_{adjust} < 0.01$, *** $p_{adjust} < 0.001$.

Figure 4 Cross-cohort comparisons of symptomatic genetic FTLD and AD

(**A**) Venn diagram showing differentially expressed proteins ($P < 0.05$) in symptomatic pathogenic variant carriers from the discovery cohort, compared with A^+T^- and A^+T^+ individuals from the Pichet Binette cohort (created in BioRender. De Houwer, J. (2025) https://BioRender.com/m8saljg). (**B**) Upset plot displaying differentially expressed proteins ($P < 0.05$) in symptomatic carriers of *MAPT*, *C9orf72*, and *GRN* variants from the discovery cohort, alongside A^+T^- and A^+T^+ individuals from the Pichet Binette cohort. The proteins unique to symptomatic *MAPT* carriers are displayed in orange. The overlap between symptomatic *MAPT* carriers, A^+T^- and A^+T^+ individuals is displayed in green.

Figure 5 Validation of the diagnostic CSF biomarker panels. (**A**) Receiver operating characteristic (ROC) curves illustrate the performance of both diagnostic panels in the validation cohort. The orange line represents the FTLD panel **A** (solid) and **B** (dotted), which distinguishes individuals with an FTLD-spectrum disorder from controls, while the red line represents the TDP panel **A** (solid) and **B** (dotted), which differentiates individuals with FTLD-TDP from controls. The area under the curve (AUC) and corresponding 95% confidence intervals (CI) are displayed. (**B**) Forest plot illustrates the different AUC and 95% CI for the FTLD panel **A** and **B** (orange), TDP panel **A** and **B** (red) and NEFL (green). To compare the performance of each panel with NEFL, we calculated ROC curves and AUC estimates for NEFL in parallel. Specifically, we generated one NEFL AUC using all FTLD individuals to match the FTLD panels, and a second NEFL AUC using only individuals with underlying TDP pathology to align with the TDP panels.

Table 1 Subject characteristics

	Discovery cohort				Validation cohort		
	Symptomatic variant carriers	**Presymptomatic variant carriers**	**Non-carriers**	***P*-value**	**FTLD**	**Controls**	***P*-value**
n	47	124	57	-	132	32	-
Age at collection, years	62 (45–81)	44 (29–75)	45 (31–72)	< 0.001	63 (32–77)	56 (31–72)	<0.001
Sex, female (%)	21 (45%)	65 (52%)	36 (63%)	0.16	58 (44%)	16 (50%)	0.16
MMSE[a]	26 (8–30)	30 (23–30)	30 (25–30)	<0.001	25 (6–30)	29 (26–30)	<0.001
CDR® plus NACC FTLD[b]	0.5: 4 1: 10 2: 10 3: 10	0: 68 0.5: 32	0: 43 0.5: 8	<0.001	0: 14 0.5: 53 1: 30 2: 4 1: 3	0 (0–0.5)	<0.001
Genetic analysis	22 *C9orf72* 14 *GRN* 10 *MAPT* 1 *TARDBP*	55 *C9orf72* 44 *GRN* 24 *MAPT* 1 *TARDBP*	-	-	18 *C9orf72* 5 *GRN* 2 *TARDBP* 54 no pathogenic variant 53 no analysis	-	-
FTLD-subtypes	37 FTLD-TDP 10 FTLD-tau	-	-	-	30 FTLD-TDP 3 FTLD-tau 99 unknown	-	-
Phenotype	36 bvFTD 5 nfvPPA 3 FTD-ALS 1 svPPA 1 PPA-NOS 1 dementia-NOS	-	-	-	49 bvFTD 11 FTD-ALS 9 nfvPPA 34 svPPA 1 lvPPA 4 PPA-NOS 17 CBS 7 PSP	-	-

Continuous variables are expressed as median (range) and were compared between groups using Kruskal-Wallis tests. Sex distributions were compared between groups using Chi-square tests. FTLD = frontotemporal lobar degeneration; MMSE = Mini Mental State Examination; CDR® plus NACC FTLD = CDR Dementia Staging Instrument plus National Alzheimer's Coordinating Center Frontotemporal Lobar Degeneration component; *C9orf72* = chromosome 9 open reading frame 72; *GRN* = progranulin; *MAPT* = microtubule-associated protein tau; *TARDBP* = TAR-DNA-binding protein; bvFTD = behavioural frontotemporal dementia; nfvPPA = non-fluent variant primary progressive aphasia; FTD-ALS = FTD with amyotrophic lateral sclerosis; svPPA = semantic variant PPA; PPA-NOS = PPA not otherwise specified; dementia-NOS = dementia not otherwise specified; lvPPA = logopenic variant PPA; CBS = corticobasal syndrome; PSP = progressive supranuclear palsy.

[a]MMSE data was available for 220 participants in the discovery cohort and for 153 participants in the validation cohort.

[b]CDR® plus NACC FTLD data was available for 189 participants in the discovery cohort and for 113 participants in the validation cohort.

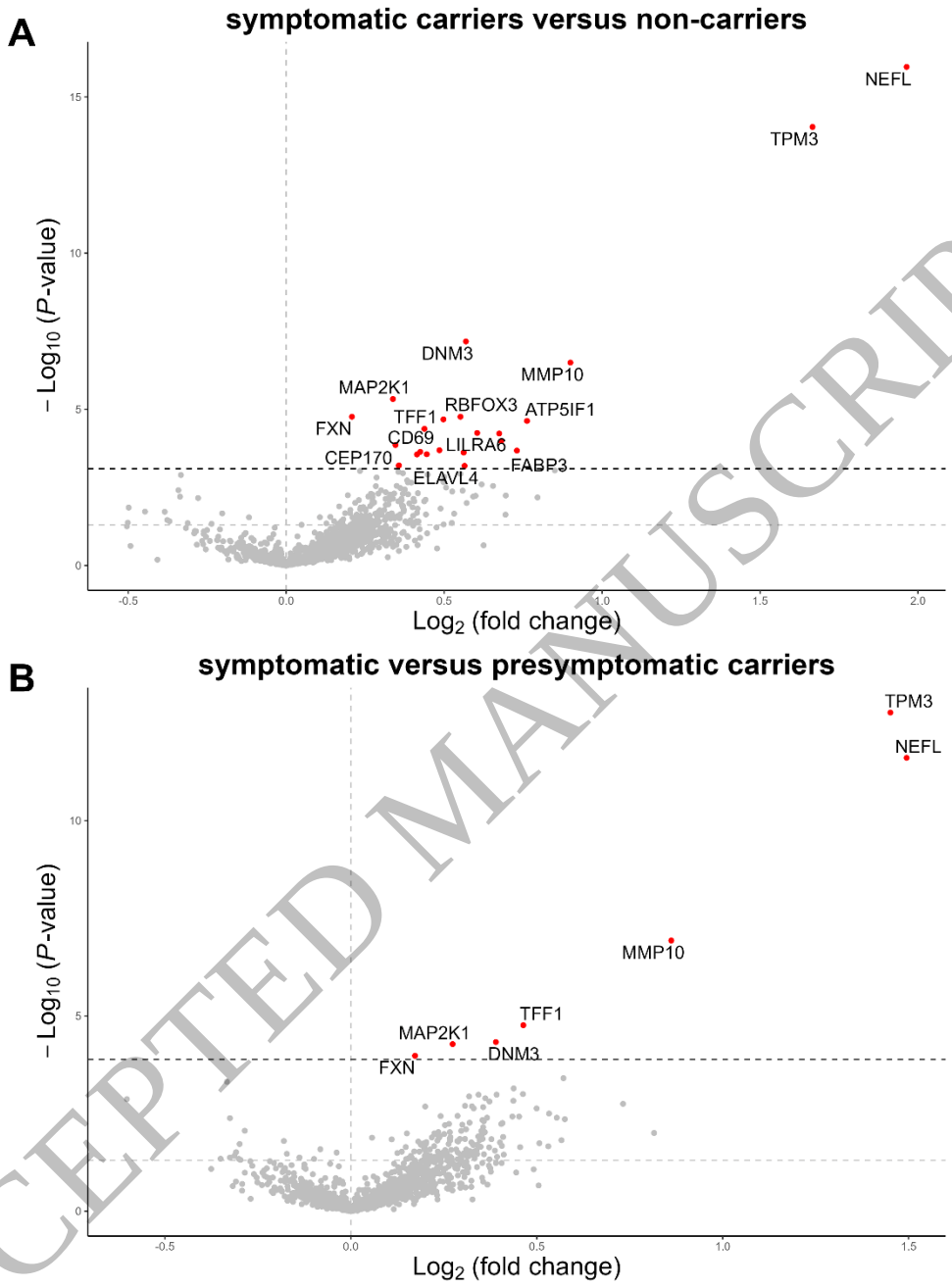

Figure 1
165x218 mm (x DPI)

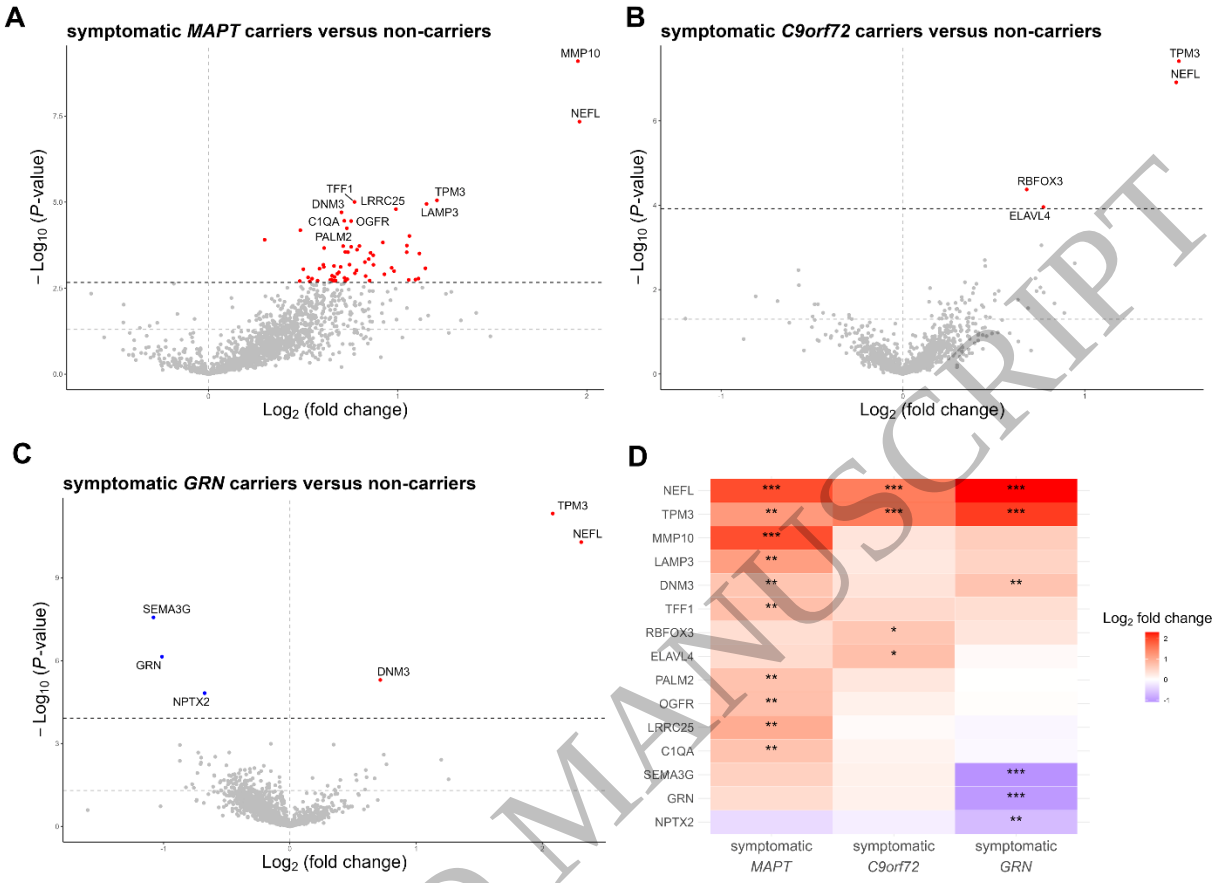

Figure 2
165x122 mm (x DPI)

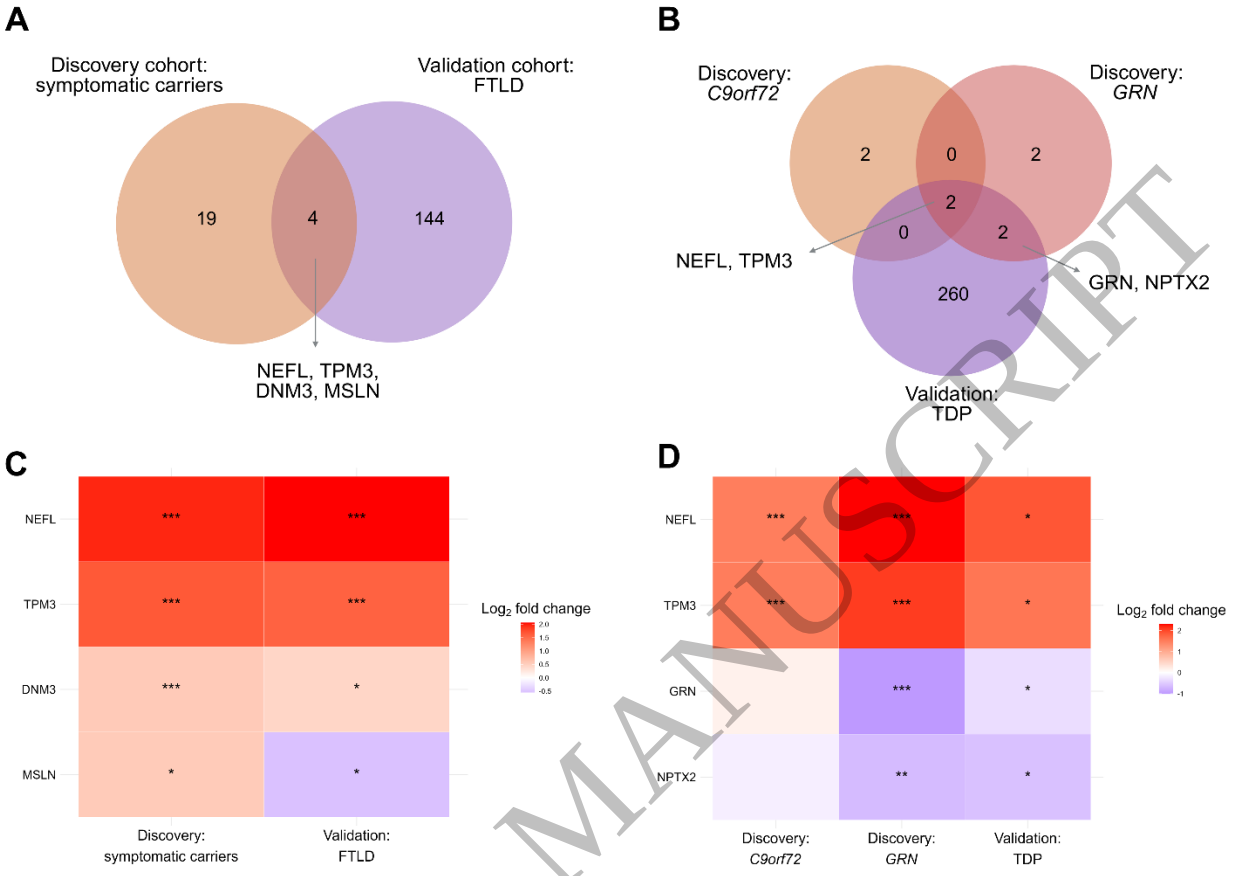

Figure 3
165x121 mm (x DPI)

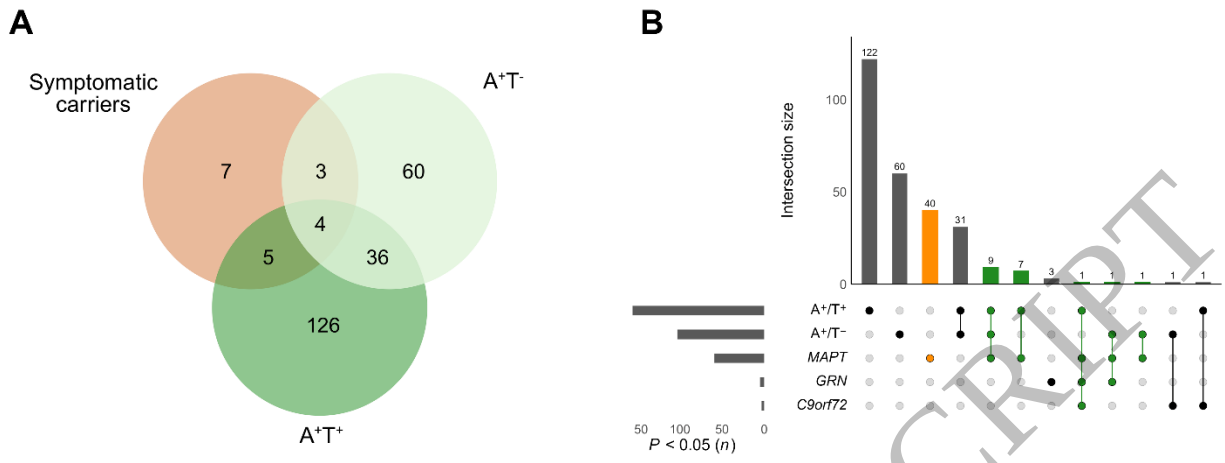

Figure 4
165x63 mm (x DPI)

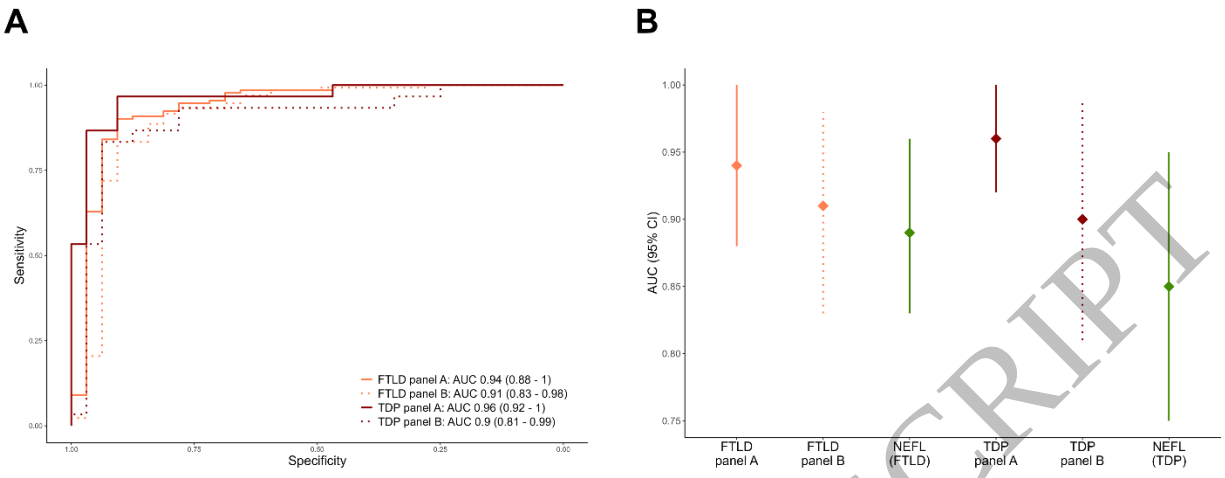

Figure 5
165x65 mm (x DPI)